Simulation of the Decay $A^0 \longrightarrow \tau^+\tau^-$ in the ATLAS Inner Detector

Peter Luthaus, Georgios Stavropoulos
Universität Dortmund, Germany

September 27, 1995

Abstract

The identification of tau-jets is an important benchmark for the performance of a tracker and the pattern recognition algorithm. This paper analyses how well the ATLAS inner detector can distinguish between tau-jets coming from decays of the pseudoscalar Higgs boson A^0 and the dominant background channels. The standard ATLAS software `SLUG/DICE` was used for the simulation and the `iPatRec` package inside `SLUG/ATRECON` for the reconstruction.

1 Introduction

The Minimal Supersymmetric Standard Model (MSSM) requires at least two Higgs doubletts to give masses to all particles. A possible selection are

$$H_1 = \begin{pmatrix} H_1^0 \\ H_1^- \end{pmatrix} \qquad \text{and} \qquad \mathrm{H}_2 = \begin{pmatrix} H_2^+ \\ H_2^0 \end{pmatrix}$$

with the vacuum expectation values v_1 and v_2. The model predicts the existence of 5 physical Higgs bosons. These are two charged bosons H^+ and H^-, two neutral scalar bosons h^0 and H^0 and one neutral CP odd boson A^0. At tree level the masses of all these Higgs bosons can be written in terms of two parameters. A possible choice are $\tan\beta = v_1/v_2$ and m_{A^0}. In higher order radiative correction arise, depending mainly on the top mass and of the squark mass at the GUT scale. For moderate values of m_{A^0} and high values of $\tan\beta$ the channel $H^0, A^0 \longrightarrow \tau^+\tau^-$ is the only process where Higgs bosons of the MSSM can be detected at the LHC [1, 2, 3]. As LEP II will not be able to cover this part of the parameter space as well, it is important to investigate how far experiments at the LHC can discover this channel.

A detailed Monte Carlo study has been done for ATLAS [2] fully simulating and reconstructing the calorimeters. Nevertheless, a complete simulation of the inner detector for this channel including pattern recognition has not been done before. This paper gives the results of a first study using the Panel layout [4] for the tracker and the `iPatRec` [5] algorithm for the reconstruction.

2 Description of the software

The events were generated with the `PYTHIA` 5.7 and `JETSET` 7.4 generators [6]. The tau polarization was inserted. The detector simulation was performed using the `SLUG/DICE` software [7, 8] which is an interface to GEANT [9]. The version of `SLUG/DICE` used for the analysis was 2.03_20 and the GEANT version was 3.21. Pattern recognition is of major importance for the analysis and this study was one of the first applications of `iPatRec`, therefore the pattern recognition software will be described in more detail.

3 Description of the pattern recognition algorithm

The `iPatRec` package is one of the algorithms one can select in `ATRECON` [10], the reconstruction interface of `SLUG/DICE`. It has already been used for a study of tau decays in the ATLAS inner detector [11].

The `iPatRec` package searches for tracks within *roads* which have to be defined by *seeds*. Within these roads it forms space points and performs a combinatorial search for tracks above a transverse momentum threshold.

For this analysis two kinds of seeds were used. These have been modified from the officially released version. One of them started with the parameters of the muon with the highest transverse momentum on generation level because

no muon reconstruction was available. The other kind of road which was used to reconstruct jets will be described in the following.

The definition of the roads is sketched in figure 1. Initially, roads were defined between the vertex and clusters in the calorimeters. As the z position of the vertex is not well known, it was searched for tracks with

$$|z_{\mathrm{vert}}| < 20\,\mathrm{cm}/\sin\theta \qquad .$$

In the transverse plane tracks had to pass within 5 mm of the origin. The half size of the roads at the calorimeters was chosen to be 0.1 in η and 0.1 in ϕ. The curvature of the roads allowed to find tracks with a minimum transverse momentum of 1 GeV.

After a first pattern recognition had been done within the roads described above, new final roads were defined. The reconstructed track with the highest transverse momentum in each road was used to restrict the z position of the vertex. Now a search for tracks with

$$z_0 - 1\,\mathrm{cm}/\sin\theta < \mathrm{z_{vert}} < \mathrm{z_0} + 1\,\mathrm{cm}/\sin\theta$$

was done, z_0 being the z coordinate of the vertex of the highest transverse momentum track. The half size of the roads at the calorimeters for this final pattern recognition was 0.3 in η and 0.4 in ϕ. The center of the roads was no longer the cluster in the calorimeters but the point where the highest momentum track intersects the calorimeters. The transverse size of the roads at the vertex remained unchanged at 5 mm.

This procedure of redefining roads and thus reducing the number of combinatorials produced better results than the default definition of the roads only for tau-jets [11].

4 Simulated Channels

The geometry of the inner detector used for this study was the so called Panel layout. The search for heavy Higgs bosons of the MSSM is considered low luminosity physics at ATLAS, especially because of the good missing transverse momentum resolution needed to reconstruct their mass. So a layer of silicon strip detectors was added 6 cm from the beam pipe. These were crossed strips with a pitch of 35 μm.

Proton-proton interactions with 14 TeV center of mass energy were simulated. The same signal and background channels as in reference [2] were used. The values used for the top mass and the squark mass are $m_t = 170$ GeV and $m_{\tilde{q}} = 1$ TeV. For the signal the following process was simulated for A^0 masses of 100, 150, 200 and 300 GeV:

$$\begin{gathered} pp \longrightarrow A^0 \, + \, X \\ A^0 \longrightarrow \tau^+ \, \tau^- \\ \tau^+ \longrightarrow \mathrm{hadrons}\, \bar{\nu}_\tau \;, \;\; \tau^- \longrightarrow \mu^- \, \bar{\nu}_\mu \, \nu_\tau \end{gathered}$$

The following backgrounds were considered:

- Z^0

$$pp \longrightarrow Z^0 + X$$
$$Z^0 \longrightarrow \tau^+ \tau^-$$
$$\tau^+ \longrightarrow \text{hadrons}\, \bar{\nu}_\tau \ , \ \ \tau^- \longrightarrow \mu^- \bar{\nu}_\mu \nu_\tau$$

- $b\bar{b}$:

$$pp \longrightarrow b\bar{b}$$
$$b \longrightarrow \text{Jets} \ , \ \ \bar{\text{b}} \longrightarrow \mu^- \bar{\nu}_\mu$$

- Top:

$$pp \longrightarrow t\bar{t}$$
$$t \longrightarrow W^+ b \ , \ \ \bar{t} \longrightarrow W^- \bar{b}$$
$$W^- \longrightarrow \mu^- \bar{\nu}_\mu \ , \ \ W^+ \longrightarrow \text{hadrons}$$

- Top Tau:

$$pp \longrightarrow t\bar{t}$$
$$t \longrightarrow W^+ b \ , \ \ \bar{t} \longrightarrow W^- \bar{b}$$
$$W^- \longrightarrow \mu^- \bar{\nu}_\mu \ , \ \ W^+ \longrightarrow \tau^+ \nu_\tau \ \ \tau^+ \longrightarrow \text{hadrons}\, \bar{\nu}_\tau$$

- W Jets

$$pp \longrightarrow W^- + \text{Jets} \ , \ \ \text{W}^- \longrightarrow \mu^- \bar{\nu}_\mu$$

The charge conjugated processed were not simulated because the cuts perform the same.

Due to limited CPU-time not all events simulated with GEANT were reconstructed. To improve the statistics, some filter cuts were applied after the generation of the events with `PYTHIA` before simulating the detector them with `SLUG/DICE`. These were the same as in reference [2] and are explained there. Table 1 lists the statistics used.

5 Analysis

The cuts performed could be separated into kinematic cuts and isolation cuts. As the statistics was too low to apply all cuts consecutively, they were done alternatively and their efficiencies multiplied.

The kinematic cuts from reference [2] were not changed compared with the analysis already done because the tracker is of minor importance for them. Here no detailed simulation for the missing p_t was done, it was calculated on particle level and smeared with the resolution given in [2]. With a low statistic, the kinematic cuts could be about reproduced.

This note focuses on the track isolation cuts by the tracker. The calorimeters were not used to support these cuts for the analysis done. Isolation cuts were performed around the highest energetic muon and around all jets which satisfied the kinematic cuts. The main kinematic cuts on jets were $p_t > 40$ GeV and $|\eta| < 2.5$. To keep an event it was necessary to have exactly one track within a cone of 0.1 in $\sqrt{\Delta\eta^2 + \Delta\phi^2}$, called acceptance cone. Additionally, no further tracks were allowed in the volume between 0.1 and 0.5, called rejection cone.

6 Results

The efficiencies of the isolation cuts are summarized in tables 2 and 3.

The $b\bar{b}$ background could be rejected by isolation criteria around the muon because the muon was generated together with a jet. Figure 2 shows the number of tracks in the vicinity of the muon for the signal and for the $b\bar{b}$ background.

Due to the low multiplicity of tau-jets all backgrounds except the Z^0 background could be rejected by isolation cuts around tau-jet candidates. The number of tracks in the area of true tau-jets of the signal and for tau-jet candidates of a representative background, the top background, are plotted in figure 3. One can see the maxima for one-prong and three-prong tau-decays.

It was shown that rejection against the background for the channel $A^0 \longrightarrow \tau^+\tau^-$ can be achieved by using track isolation cuts with the tracker. Nevertheless, these cuts perform a lot worse than the calorimeter cuts in reference [2]. Their power is insufficient to observe any signal without adding more cuts.

7 Conclusions and outlook

A slight improvement of the significance can be expected by using not only one-prong decays but also three-prong decays of the taus and applying cuts related to a reconstructed vertex.

The analysis in reference [11] has shown that, especially in the forward direction, the pattern recognition efficiencies of the Panel layout are not satisfactory. In the mean time new geometries for the tracker have been proposed which promise better pattern recognition performance, the *Annecy* and *Morges* layouts.

Additionally, further development is needed to improve the pattern recognition algorithms. The `iPatRec` algorithm was still in a phase of development and future releases are expected to perform better. Improvements that have been done in the meantime include the treatment of errors for low energetic tracks which should allow to make vertex cuts for three-prong decays.

Another option is to develop a slightly different strategy for pattern recognition based on pixel detectors. To support such an algorithm currently a layout of the ATLAS detector with replacing one or two layers of strip detectors by large pixel detectors is studied.

In future studies the combined performance of tau-jetcuts fully simulating a more actual layout of the tracker and the calorimeters could be done. This will give a more realistic assessment for the capability of the ATLAS detector to investigate the channel $A^0 \longrightarrow \tau^+\tau^-$ than only simulating parts of the detector.

Acknowledgements

We are thankful to Donatella Cavalli, Claus Gößling and Alan Poppleton for discussions and support.

References

[1] Z. Kunszt and F. Zwirner, *Nucl. Phys.* **B385** (1992) 3.

[2] D. Cavalli et al., ATLAS Internal Note INDET-NO-051 (1994).

[3] ATLAS Technical Proposal CERN/LHCC/94-43, LHCC/P2 (1994).

[4] The ATLAS collaboration, progress report on ATLAS milestones, CERN/LHCC/94-22.

[5] R. Clifft and A. Poppleton, ATLAS Internal Note SOFT-No-009 (1994).

[6] T. Sjöstrand, PYTHIA 5.7 and JETSET 7.4, Physics and Manual, CERN-TH.7112/93.

[7] R. S. DeWolf, Slug Manual (1993).

[8] DICE Manual (0.10) (1994).

[9] GEANT, Detector Description and Simulation Tool, CERNLIB Long Writeup W5013.

[10] DRAFT ATLAS ATRECON manual (0.015) (1994).

[11] P. Luthaus et al., ATLAS Internal Note INDET-NO-099 (1995).

channel	gen.	sim.	reconst.
A^0 100 GeV	34495	2085	1228
A^0 150 GeV	7929	1623	1178
A^0 200 GeV	7199	2355	1984
A^0 300 GeV	3842	1895	936
Z^0	188936	4971	907
$b\bar{b}$	831413	1966	1246
Top	6618	1321	591
Top Tau	11588	1953	1185
W Jets	133512	2581	644

Table 1: Number of generated, simulated and reconstructed events

Channel	Efficiency [%]	Rejection [%]
A^0 100 GeV	93 ± 1	
A^0 150 GeV	93 ± 1	
A^0 200 GeV	92 ± 1	
A^0 300 GeV	90 ± 1	
Z^0		4 ± 1
$b\bar{b}$		97.5 ± 0.6
Top		16 ± 2
Top Tau		12 ± 1
W Jets		6 ± 1

Table 2: Efficiency of the isolation cuts around the muon

Channel	Efficiency [%]	Rejection [%]
A^0 100 GeV	25 ± 1	
A^0 150 GeV	37 ± 1	
A^0 200 GeV	41 ± 1	
A^0 300 GeV	45 ± 2	
Z^0		69 ± 2
$b\bar{b}$		98.9 ± 0.4
Top		97.5 ± 0.7
Top Tau		88 ± 1
W Jets		98.3 ± 0.7

Table 3: Efficiency of the isolation cuts around the tau-jet candidates

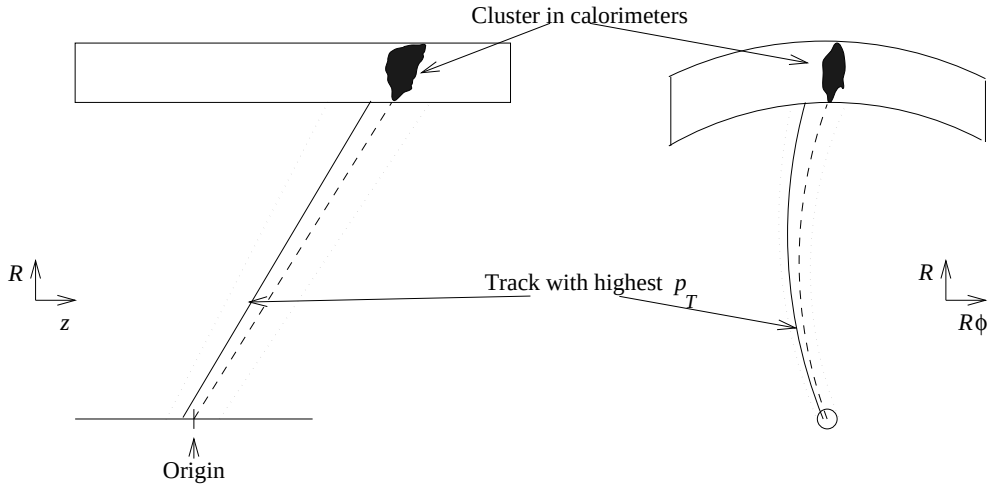

Figure 1: Definition of the roads used to reconstruct jets (not to scale). Dashed lines show the centers of the roads, dotted lines their boundaries. Solid lines connecting the vertex region and the calorimeters represent the track with the highest transverse momentum reconstructed after pattern recognition in the initial roads.

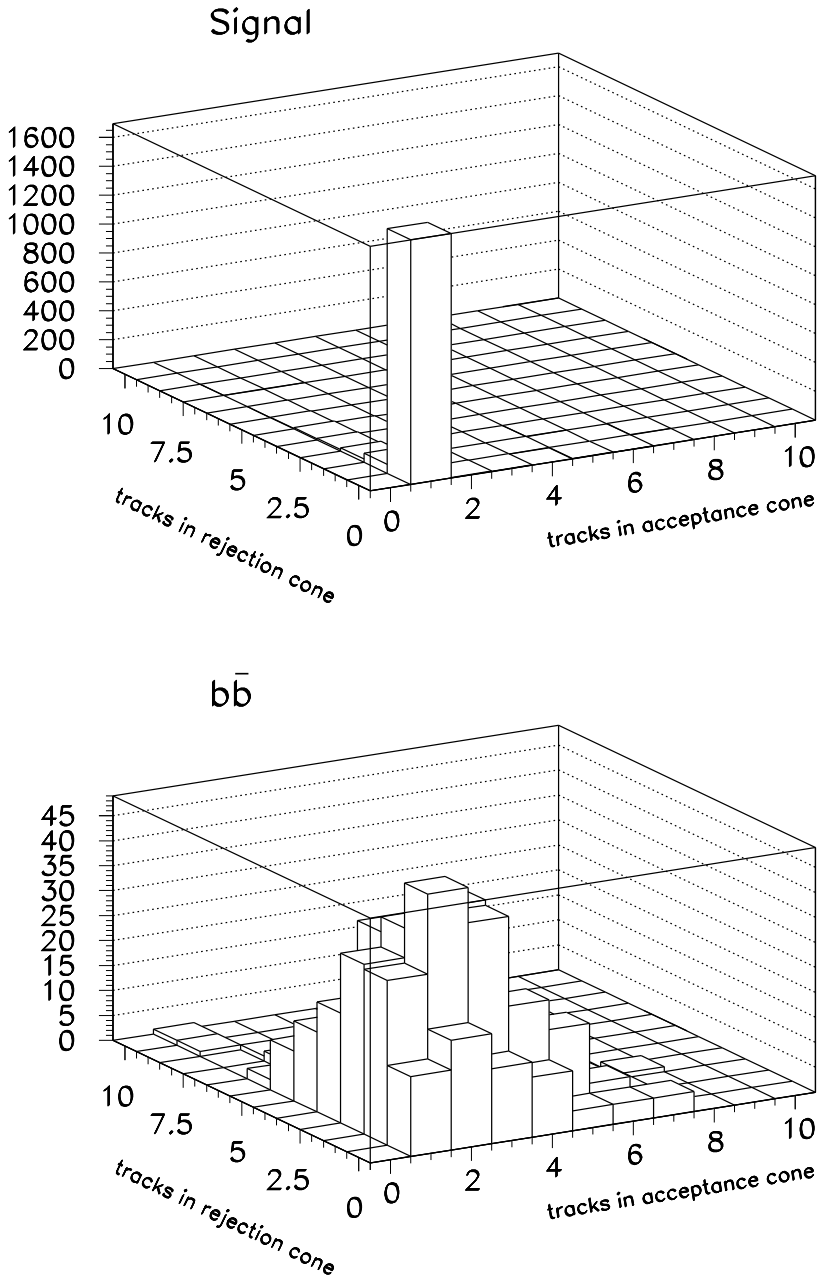

Figure 2: Number of tracks in the vicinity of the highest energetic muon for the signal with $m_A = 200$ GeV and the $b\bar{b}$ background

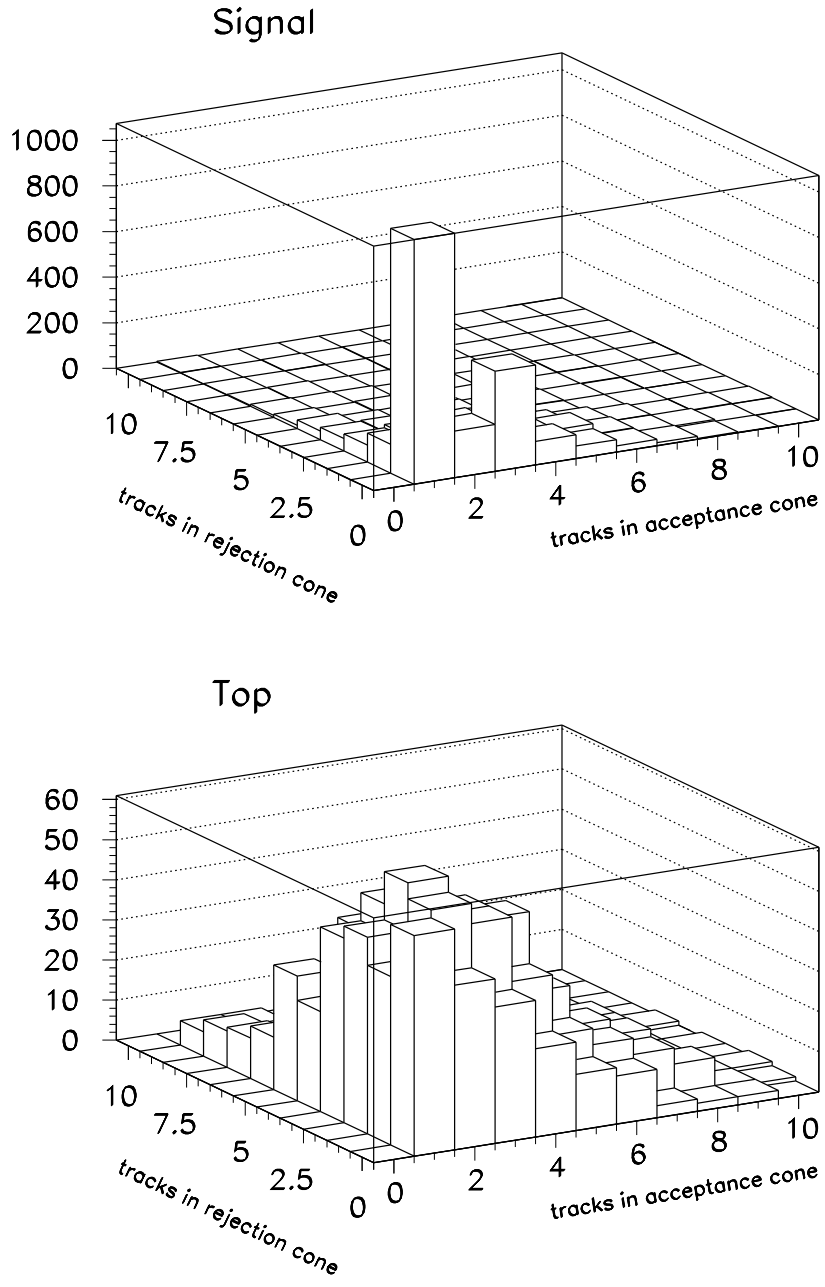

Figure 3: Number of tracks in the vicinity of true tau-jets for signal with $m_A = 200$ GeV and for tau-jet candidates after kinematic cuts from the top background